Spatial Distribution of Electrochemical Performance in a Planar Segmented SOFC

Günter Schiller[1]*, Caroline Willich[1], K. Andreas Friedrich[1], Stefan Gewies[2], Nicolas Bayer Botero[2], Wolfgang G. Bessler[1,2]

[1] Deutsches Zentrum für Luft- und Raumfahrt (DLR)
Institut für Technische Thermodynamik
Pfaffenwaldring 38-40
D-70569 Stuttgart / Germany
* Tel: +49-711 6862635
guenter.schiller@dlr.de

[2] Universität Heidelberg
Interdisziplinäres Zentrum für Wissenschaftliches Rechnen (IWR)
Im Neuenheimer Feld 368
D-69120 Heidelberg / Germany

Abstract

Spatially inhomogeneous distributions of current density and temperature in solid oxide fuel cells (SOFC) can contribute significantly to accelerated electrode degradation, thermomechanical stresses, and reduced efficiency. This is particularly the case under technically relevant operating conditions, that is, high fuel utilization. A combined experimental and modeling study of the spatial distribution of the electrochemical performance in a planar SOFC was performed in order to determine local effects and to identify critical operating conditions.

A planar anode-supported SOFC single cell was locally characterized in a 4×4-segmented cell arrangement. The tests were performed in counter flow operation for various $H_2/H_2O/N_2$ mixtures at the anode and O_2/N_2 mixtures at the cathode. Local and global current-voltage relationships were measured in dependence of gas composition and fuel utilization. A two-dimensional elementary kinetic electrochemical model representing the segmented cell along the flow path and through the thickness of membrane-electrode assembly and interconnector was established. It reflects the experimental setup in a highly detailed way and allows to quantitatively interpret experimental observations. The model was validated by comparison to experiments under a wide range of operating conditions.

When the cell was operated at high fuel utilization, both measurements and simulations show a strong variation of the electrochemical performance along the flow path. The simulations predict a considerable gradient of gas-phase concentrations along the fuel channel and through the thickness of the porous anode, while the gradients are lower at the cathode side. It is expected that the anode is more susceptible to spatially inhomogeneous degradation than the cathode.

Introduction

In order to achieve optimum fuel cell performance and minimum degradation, a homogeneous electrochemical activity and temperature over the whole area of the electrodes is required. Inhomogeneous distributions of current density and temperature result in a reduced utilization of the reactants or the catalyst and, hence, in reduced efficiency. Furthermore, long-term stability of cell components are likely to be detrimentally affected by an inhomogeneous distribution of the electrical and thermal properties in the cell. For this reason, it is highly desirable to obtain detailed information about the spatial distribution of the electrical, chemical and thermal cell properties. For polymer electrolyte fuel cells (PEFC), different setups for the local measurement of particularly the current density distribution have been developed and are widely used [1-7]. In contrast to this, only few experiments for a spatially resolved characterization of solid oxide fuel cells (SOFC) have been conducted so far, mainly because the high operating temperature represents a considerable challenge to the experimental setup. One of the first and most powerful setups for the local characterization of segmented SOFC cells has been developed at DLR Stuttgart [8-12] .

A more fundamental understanding of the complex behavior in cells in dependence of the local operating conditions can be achieved by combining experimental investigations with modeling studies. A two-dimensional electrochemical model representing the segmented cell along the flow path and through the thickness of the membrane-electrode assembly and interconnect has been established at the University of Heidelberg [13,14]. The model includes the description of gas-phase mass and heat transport in the interconnect channels and in the porous electrodes, the elementary kinetic heterogeneous and charge-transfer reactions in the electrodes, as well as mass and charge transfer in the membrane-electrode assembly. The model thus reflects the experimental setup in a highly detailed way and allows to quantitatively interpret the experimental observations.

Here we present first results from a combined experimental and modeling study of the spatial distribution of the electrochemical performance in a planar SOFC. Goal of the study is the determination of local effects and identification of critical operating conditions during technically relevant SOFC operation.

Experimental

The measurement setup for segmented cells is shown schematically in Fig. 1. It allows for the integral and spatially resolved measurement of current density and voltage, the local and integral determination of impedance data, the local measurement of temperature and temperature distribution and the spatially resolved analysis of the fuel gas concentrations along the flow path. Square-shaped cells with an area of 100 cm² are divided into 16 segments with an active area of 4.84 cm² of each segment. The cells are integrated in a metallic cell housing and sealed with glass seal provided by Fraunhofer Institute of Ceramic Technologies and Sintered Materials (IKTS) in Dresden, Germany. The metallic housing is subdivided into 16 galvanically isolated segments with a total active area of 73.96 cm². In order to determine the temperature at each segment, thermocouples are introduced in the metallic segments. Additionally, capillary tubes that correspond to the cathodic segments are integrated at the anode side at 16 measuring points to take samples of the anode gas to be analyzed by gas chromatography.

The setup is flexible with regard to the integration of different cell designs. Metal-supported cells (MSC), as they are developed and fabricated in house according to the DLR spray concept, as well as electrolyte-supported cells (ESC) and anode-supported cells (ASC) can be characterized. With MSC and ASC, only the cathode is segmented, whereas ESC are segmented on both the anode and the cathode side. The anode-supported cells used in this investigation contained a 540 µm thick NiO/YSZ anode with a thin anode functional layer, a 7 µm thick 8YSZ electrolyte, a 7 µm thick YDC interlayer and a 30 µm thick LSCF cathode. For the contact of the electrodes Ni and Pt meshes were used. More details on the measurement system are given in [8,9].

Modeling and Simulation

A detailed two-dimensional multi-scale elementary kinetic electrochemical model was developed that represents one single channel of the experimental setup. The model layout is shown schematically in Fig. 2. The structural and operational model parameters are summarized in Table 1. The modeling approach was presented in detail in [13] and is only summarized here. One-dimensional channel flow (*x* dimension) is described using the Navier-Stokes conservation equations (continuity, species, momentum). One-dimensional transport through the MEA (*y* dimension) is described by coupled mass transport (Fickian and Knudsen diffusion, Darcy flow) and charge transport (Ohm's law for the electrolyte). The results shown in this paper are calculated under the assumption of isothermal conditions.

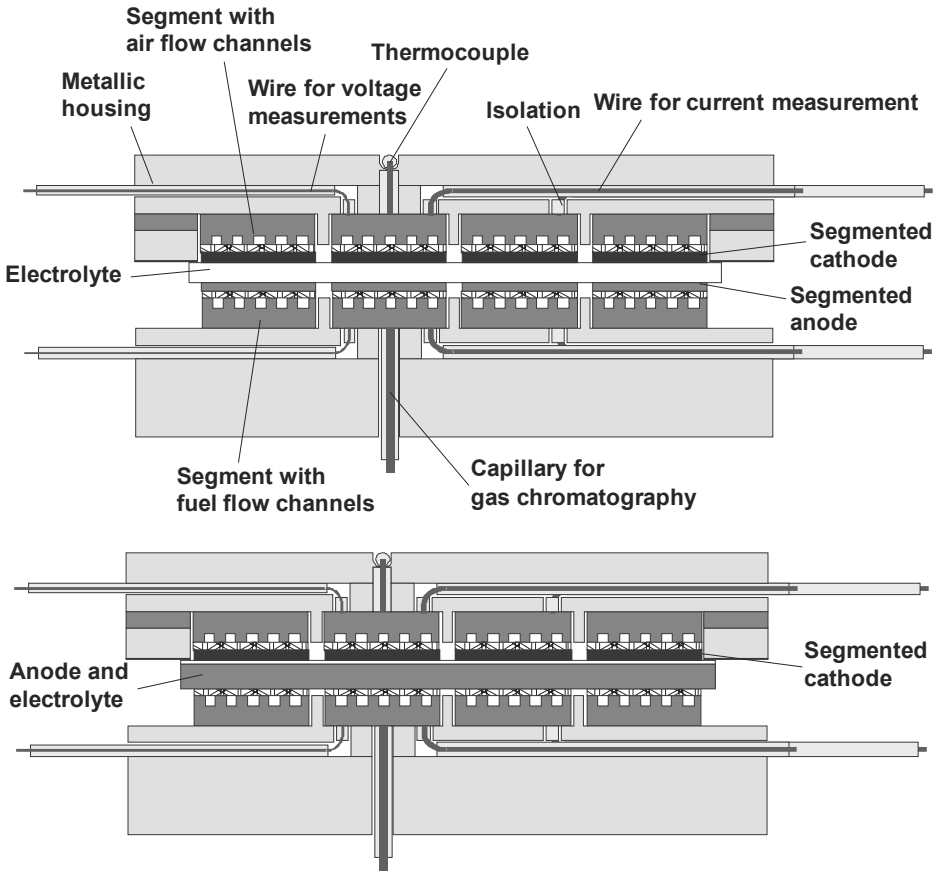

Fig. 1: Setup of measurement system for the characterization of segmented cells:
(a) Housing with anode and cathode segmentation used for electrolyte-supported cells
(b) Housing with cathode segmentation used for metal- and anode-supported cells.

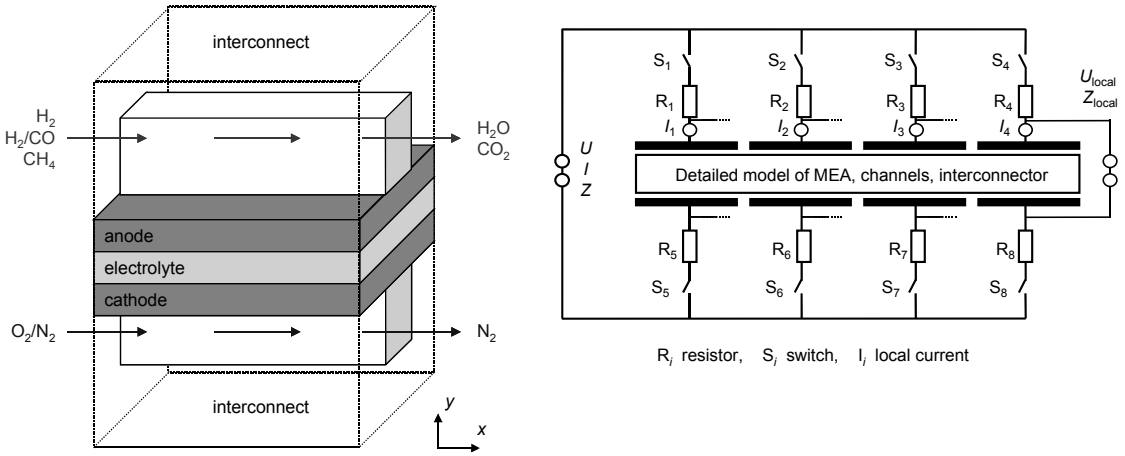

Fig. 2: Model of the segmented SOFC. Left: two-dimensional representation of one single gas channel including MEA and interconnect. Right: representation of segmentation by an electrical circuit.

Model parameter	Value	Ref.
Gas channel		
Length L_{cha}	9.8 cm	Setup
Channel cross-sectional area A_{cha}	4 mm^2	Setup
Channel perimeter P_{chem}	4 mm	Setup
Segmented cell		
Number of segments in one channel	4	Setup
Segment area	2.2 cm x 2.2 cm	Setup
Inactive region between segments	0.2 cm	Setup
Porous media (mesh anode, cermet anode, porous cathode, mesh cathode)		
Layer thickness: $D_{mesh,a}$, D_{anode}, $D_{cathode}$, $D_{mesh,c}$	450 µm, 540 µm, 70 µm, 490 µm	Setup
Porosity: $\varepsilon_{mesh,a}$, ε_{anode}, $\varepsilon_{cathode}$, $\varepsilon_{mesh,c}$	0.74, 0.32, 0.40[a], 0.82	Setup [17]
Pore size: $d_{mesh,a}$, d_{anode}, $d_{cathode}$, $d_{mesh,c}$	100 µm, 0.7 µm, 0.7 µm[a], 125 µm	Setup
Tortuosity: $\tau_{mesh,a}$, τ_{anode}, $\tau_{cathode}$, $\tau_{mesh,c}$	1.5[a], 3.6[b], 3.8[b], 1.5[a]	[a] Estimated [b] Fitted
Cermet anode parameter		
Active three-phase boundary length L_{TPB}	$4.2 \cdot 10^{12}$ m/m^3	Microstructrual model [14]
Effective width electrolyte w_{YSZ}	0.26 µm	
Effective width electrode w_{Ni}	0.54 µm	
Structural factor electrolyte conductivity f_σ	0.129	
Electrolyte		
Thickness D_{YSZ}	14 µm	Setup
Conductivity bulk 8YSZ A_σ, E_σ	$5.15 \cdot 10^7$ SK/m, 84 kJ/mol	[18]
Contact resistance		
Anode and cathode	0.03 Ωcm^2	[17]
Conditions		
Temperature T	700 - 850 °C	Exp.
Pressure p	1013 hPa	Exp.
Anode gas phases H_2, H_2O, N_2		Exp.
Cathode gas phases O_2, N_2		Exp.

Table 1: Model parameters

Anode electrochemistry is described using elementary kinetics for surface reactions on Ni and YSZ, and for charge transfer (hydrogen spillover) [15]. The reaction mechanism is given in Table 2. Cathode electrochemistry is described using a modified Butler-Volmer equation given in [13] as derived by Zhu et al. [16]. Current-voltage relationships are modeled by directly solving for the electric-potential distribution in the electrodes and electrolytes without using the Nernst equation. The segmentation is represented by an electrical circuit model where an arbitrary number of segments can be used. All models are implemented in the in-house numerical simulation software DENIS.

Anode Reaction	Preexp. factor k_f	Activation en. E_f^{act}
Charge transfer reaction (Fit):		
$H_{Ni} + OH^-_{YSZ} \rightleftharpoons \square_{Ni} + H_2O_{YSZ}$	$5.64 \cdot 10^5$ mol/(m s) [a]	235 kJ/mol [b]
YSZ surface reactions:		
$H_2O + \square_{YSZ} \rightleftharpoons H_2O_{YSZ}$	S = 1 (sticking coeff.)	–
$H_2O_{YSZ} + O^{2-}_{YSZ} \rightleftharpoons 2\ OH^-_{YSZ}$	$1.6 \cdot 10^{22}$ cm^2/(mol s)	9.6 kJ/mol
$O^x_{O\,YSZ} + \square_{YSZ} \rightleftharpoons V^{\bullet\bullet}_{O\,YSZ} + O^{2-}_{YSZ}$	$1.6 \cdot 10^{22}$ cm^2/(mol s)	91 kJ/mol
Nickel surface reactions:		
$H_2 + 2\ \square_{Ni} \rightleftharpoons 2\ H_{Ni}$	*S* = 0.1 (sticking coeff.)	–
$H_2O + \square_{Ni} \rightleftharpoons H_2O_{Ni}$	*S* = 0.01 (sticking coeff.)	–
$H_{Ni} + O_{Ni} \rightleftharpoons OH_{Ni} + \square_{Ni}$	$5.0 \cdot 10^{22}$ cm^2/(mol s)	98 kJ/mol
$H_2O_{Ni} + O_{Ni} \rightleftharpoons 2\ OH_{Ni}$	$5.4 \cdot 10^{23}$ cm^2/(mol s)	209 kJ/mol
$H_{Ni} + OH_{Ni} \rightleftharpoons H_2O_{Ni} + \square_{Ni}$	$3.0 \cdot 10^{20}$ cm^2/(mol s)	43 kJ/mol

Cathode Reaction	Exchange current density i^0
$O_2 + 2\,V^{\bullet\bullet}_{O\,YSZ} + 4\ e^- \rightleftharpoons 2\ O^x_{O\,YSZ}$	$2.8 \cdot 10^5$ A/m^2 [a]

[a] Fitted to the present experiments.
[b] Fitted to experiments with symmetrical SOFC anodes [14].

Table 2: Elementary kinetic reaction mechanism for the anode [15] and global kinetic reaction for the cathode. A single hydrogen spillover between Ni and YSZ surfaces is assumed as active charge-transfer reaction. A symmetry factor α = 0.5 is assumed. The surface site densities of Ni and YSZ are $3.2 \cdot 10^{-9}$ and $6.3 \cdot 10^{-10}$ mol/cm^2, respectively.

Results and Discussion

Measurement Example

Fig. 3a shows exemplarily spatially resolved IV-characteristics monitored at 800 °C operating temperature along the flow path in a segment row as indicated in Fig. 3b. The local voltages differ significantly from the fuel inlet (segment 9) to the fuel exit (segment 12) particularly at high global current densities above approximately 700 mA/cm^2. The gas flow rates were 25 smlpm/cm^2 for the anode and 80 smlpm/cm^2 for the cathode gases; the fuel utilization was 60%.

Model Validation and Parameter Identification

There are a number of model parameters associated with electrochemistry and transport in the MEA that are specific for the investigated cells and cannot be obtained from independent literature. Some parameters can be reliably estimated (e.g., porosity from SEM micrographs). Other parameters, however, can only be obtained by fitting to experimental data. Here, we use the electrochemical performance of anode and cathode (preexponential factors, activation energies) as well as porous electrode tortuosities as free parameters. These parameters were fitted and the model validated under specifically designed operating conditions: Experimental polarization behavior was measured under low fuel utilization (< 10 % by using fast gas inflow velocities) in order to circumvent spatial gradients along the channel. Gas-phase anode and cathode inlet concentrations as well as temperature were varied over a wide range of conditions (gas composition, gas dilution, temperature); these conditions were chosen in order to achieve sensitivity for the unknown parameters. The model parameters were fitted using an isothermal one-dimensional model of the MEA only. Fitting results are included in Tables 1 and 2.

Simulated and experimental polarization curves for the validation conditions are shown in Fig. 4. There is overall good agreement between model and experiment over the complete range of operating conditions. However, a systematic deviation between model and experiment occurs in Fig. 4d and e. We believe that this is due to an onset of cell degradation, lowering the experimentally observed performance relative to the model predictions. Note that one single set of model parameters was used for all conditions. Degradation effects are not included in the model.

(a) (b)

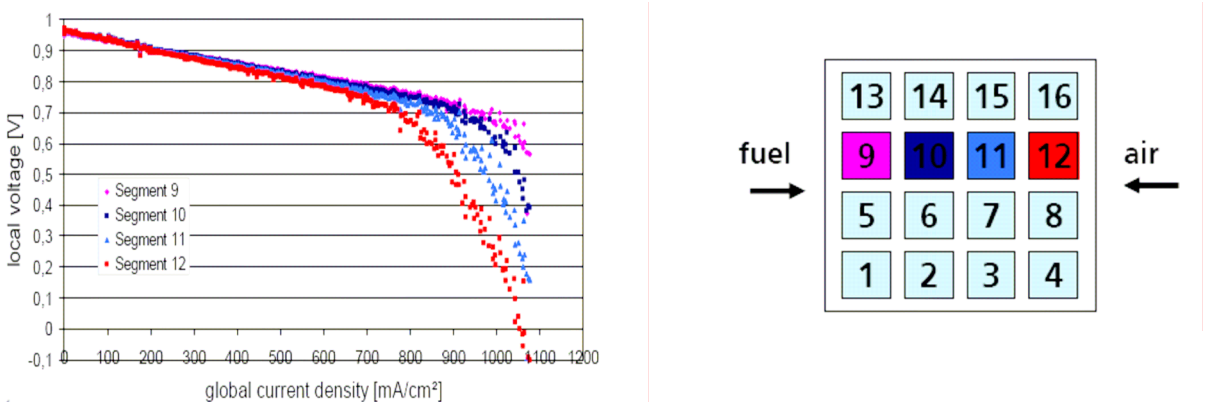

Fig. 3: IV-characteristics of segments 9 to 12 with anode $X(H_2)$: $X(H_2O)$ = 50 : 50 and cathode $X(O_2)$: $X(N_2)$ = 50 : 50 (a); segmentation of the cell (b)

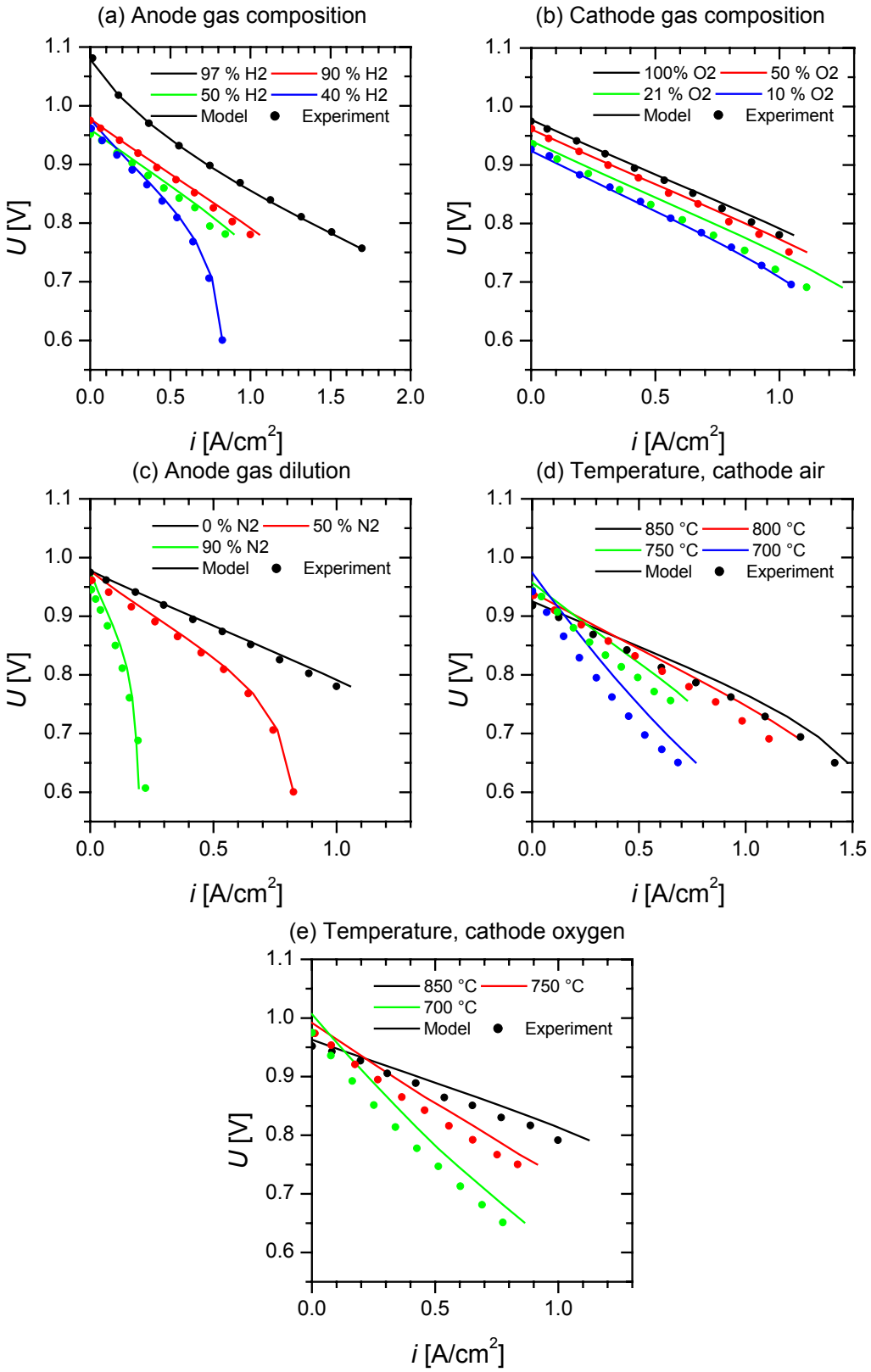

Fig. 4: Comparison of experimental data under validation conditions (low fuel utilization) and 1D model calculations. (a) Variation of anode gas composition with $X(N_2)$ = 0 at 800 °C with cathode 100 % O_2; (b) Variation of cathode gas composition at 800 °C with anode $X(H_2)$: $X(H_2O)$: $X(N_2)$ = 50 : 50 : 0; (c) Variation of anode gas composition with $X(H_2)$: $X(H_2O)$ = 1 : 1 at 800 °C with cathode 100 % O_2; (d) Variation of temperature with anode $X(H_2)$: $X(H_2O)$: $X(N_2)$ = 50 : 50 : 0 and cathode air; (e) Variation of temperature with anode $X(H_2)$: $X(H_2O)$: $X(N_2)$ = 50 : 50 : 0 and cathode 100 % O_2.

Full Simulation Predictions

The segmented planar cell was simulated with the full 2D model using the validated parameters obtained from the 1D model. For the simulations performed here, a realistic operating condition under high fuel utilization was assumed. The anode was fed with 90 % H_2/10 % H_2O at 1 m/s channel inflow velocity, corresponding to a maximum current density of 2.2 A/cm^2. The cathode was fed with air at 6.5 m/s channel inflow velocity, corresponding to a maximum current density of 6.8 A/cm^2. Counter-flow operation was assumed, and temperature was set to 800 °C.

Simulated global and local current-voltage characteristics for this condition are shown in Fig. 5. The global IV-curve (Fig. 5a) shows a typical shape with an almost linear behavior at low currents and a limiting current density of ~1.6 A/cm^2. This is less than the value resulting from the H_2 influx (2.2 A/cm^2). The limiting current density observed here is therefore not due to full fuel utilization, but due to diffusion losses in the porous anode. The local IV-curves can be represented in different ways by either plotting local voltage versus local current (Fig. 5b) or cell voltage versus local current (Fig. 5c). In the first representation, the contact resistance between electrode and current collector contributes individually to the segment voltages. The local behavior shows a considerable variation of the limiting current density for different cell segments.

Fig. 6 shows the simulated spatially resolved distributions of gas-phase concentrations in the interconnector channels as well as in the porous electrodes and current collector meshes for a global current density of 1.3 A/cm^2. This condition corresponds to the condition of maximum power density; the fuel utilization is 59 %. There are considerable concentration gradients throughout the complete system. In particular, the relatively thick porous anode in this anode-supported cell is responsible for strong H_2 depletion through the anode thickness. The upper panel of Fig. 6 also shows the local current density along the flow path. The step-like behavior over the four segments is obvious.

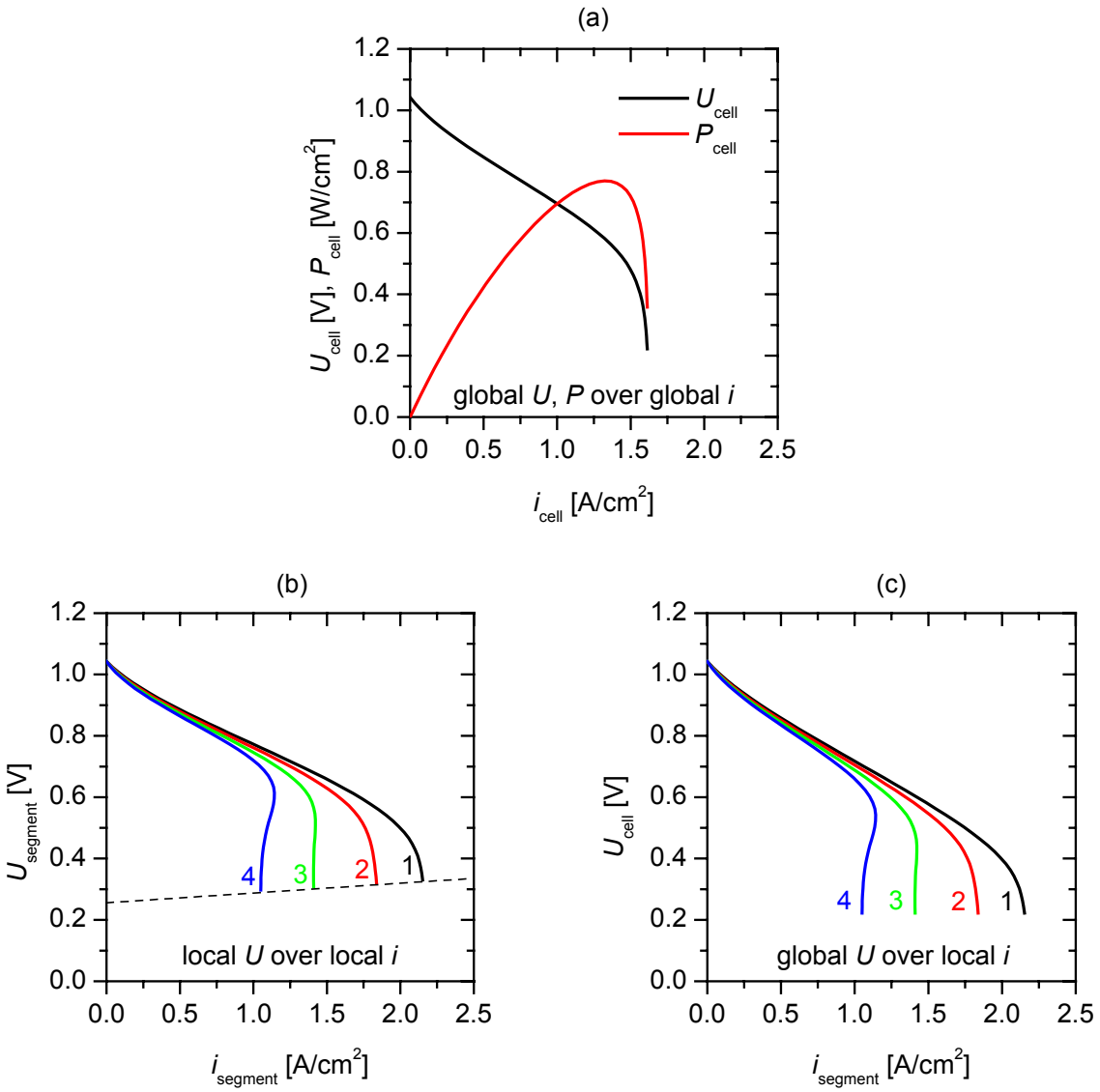

Fig. 5: Simulated polarization behavior for the segmented cell using the full 2D model under realistic operating conditions (counter-flow operation; anode: 10 % H_2O in H_2, 1 m/s inflow velocity; cathode: air, 6.5 m/s inflow velocity; T = 800 °C). The numbers indicate the segments, where segment 1 is the first in flow direction of the fuel gas. (a) Global current-voltage curves. (b) Local segment voltage versus local segment current. (c) Global cell voltage versus local segment current. The dashed line connects points of equal global cell voltage. It represents the polarization losses due to contact resistance.

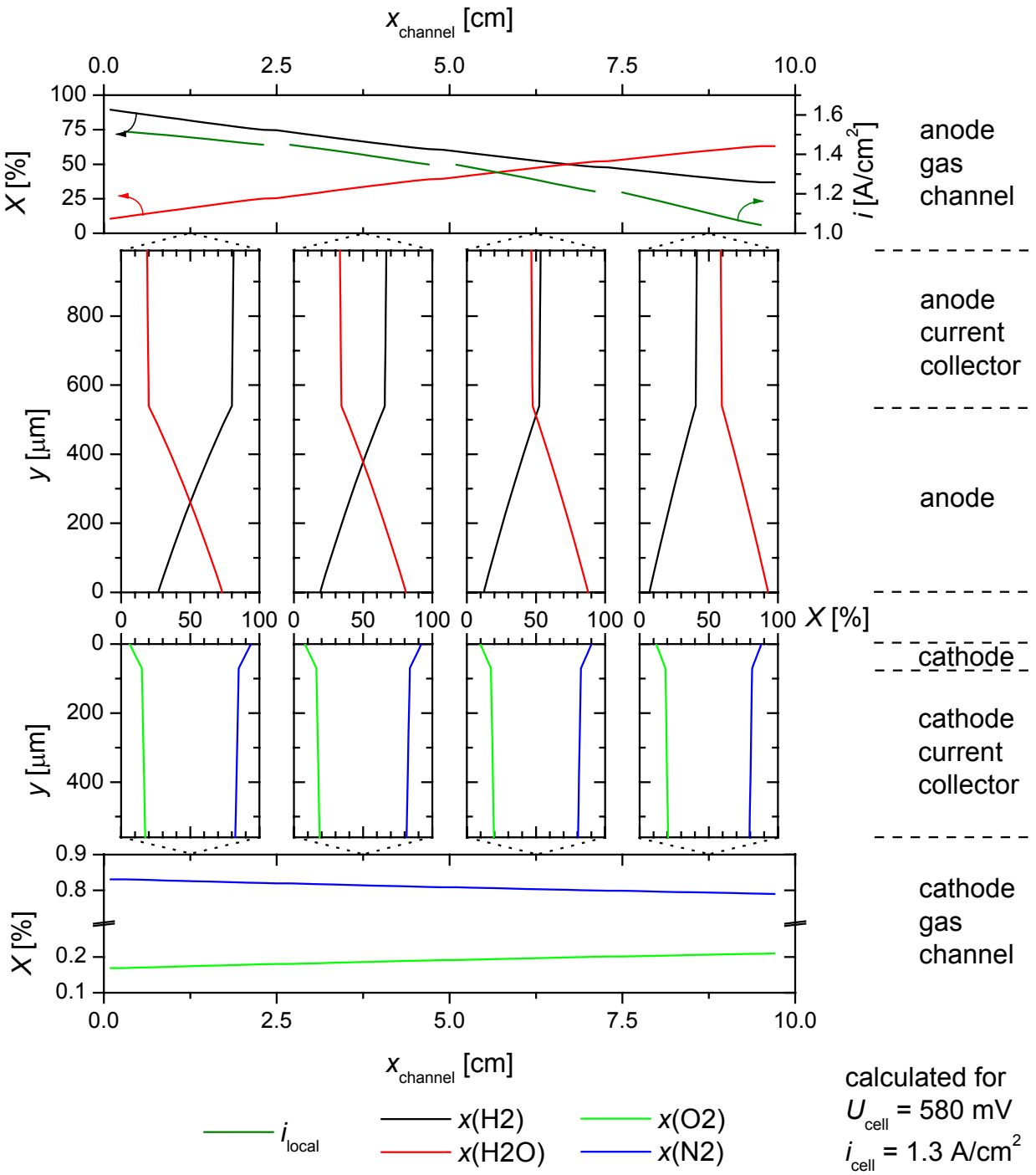

Fig. 6: Distribution of local current density and gas-phase concentrations within channel and porous electrodes on anode and cathode side for a global cell current density of 1.3 A/cm^2, corresponding to a fuel utilization of 59 % (point of maximum power density).

Conclusions

A combined experimental and modeling study of the spatial distribution of the electrochemical performance in a planar SOFC was performed. Experimental data were obtained using a specifically designed segmented cell setup that allows the measurement of local current-voltage characteristics, gas composition and temperature. Simulations were performed using a two-dimensional elementary kinetic model that represents the experimental setup.

In this paper we have presented first results from this combined study. Model parameters were identified by comparing simulations with validation experiments under low fuel utilization. A good agreement between simulation and experiment was observed. Simulations of the cell under realistic operating conditions showed strong gradients of gas concentrations and current density along the flow path and throughout the thickness of the membrane-electrode assembly. The relatively thick porous anode and high fuel utilization causes particularly strong concentration variations at the anode, while the gradients are lower at the cathode side. We would therefore expect the anode to be more susceptible to spatially inhomogeneous degradation than the cathode.

Acknowledgements

Funding was provided by the Umweltministerium Baden-Württemberg, Germany, through the programme “Herausforderung Brennstoffzelle”.

References

1. M. Noponen, T. Tennola, M. Mikkola, T. Hottinen, and P. Lund, "Measurement of current distribution in a free-breathing PEMFC," J. Power Sources **106**, 304-312 (2002).
2. D. J. L. Brett, S. Atkins, N. P. Brandon, V. Vesovic, N. Vasileiadis, and A. R. Kucernak, "Measurement of the current distribution along a single flow channel of a solid polymer fuel cell," Electrochemistry Communications **3**, 628-632 (2001).
3. N. Rajalakshmi, M. Raja, and K. S. Dhathathreyan, "Evaluation of current distribution in a proton exchange membrane fuel cell by segmented cell approach," J. Power Sources **112**, 331-336 (2002).
4. G. Bender, M. S. Wilson, and T. A. Zawodzinski, "Further refinements in the segmented cell approach to diagnosing performance in PEFC," J. Power Sources **123**, 163-171 (2003).
5. S. Schönbauer and H. Sander, "Experimental Investigation of Current Density Distribution in Polymer Electrolyte Fuel Cells," in *Proceedings of the 3rd European PEFC Forum*, Lucerne, Switzerland, B056 (2005).
6. I. A. Schneider, S. A. Freunberger, D. Kramer, A. Wokaun, and G. G. Scherer, "Oscillations in gas channels. Part I. The forgotten player in impedance spectroscopy in PEFCs," J. Electrochem. Soc. **154**, B383-B388 (2007).
7. M. Schulze, E. Gülzow, S. Schönbauer, T. Knöri, and R. Reissner, "Segmented Cells as Tool for Development of Fuel Cells and Error Prevention/Prediagnostic in Fuel Cell Stacks," J. Power Sources **173**, 19-27 (2007).
8. P. Metzger, G. Schiller, and A. O. Störmer, "SOFC Characteristics Along the Flow Path," in *Proceedings of the 6th European Solid Oxide Fuel Cell Forum*, Lucerne, Switzerland, 989-999 (2004).

9. P. Metzger, K.-A. Friedrich, H. Müller-Steinhagen, and G. Schiller, "SOFC characteristics along the flow path," Solid State Ionics **177**, 2045-2051 (2006).
10. P. Metzger, K. A. Friedrich, G. Schiller, and H. Müller-Steinhagen, "Investigation of Locally Resolved SOFC Characteristics Along the Flow Path," ECS Transactions **7**, 1841-1847 (2007).
11. P. Metzger, K. A. Friedrich, G. Schiller, and H. Müller-Steinhagen, "Investigation of Locally Resolved SOFC with Respect to Flow Configurations and Gas Compositions," ECS Transactions (2008).
12. P. Metzger, K. A. Friedrich, G. Schiller, and C. Willich, "Spatially Resolved Measuring Technique for SOFC," in *Proceedings of the 2nd European Fuel Cell Technology and Application Conference*, Rome, Italy (2007).
13. W. G. Bessler, S. Gewies, and M. Vogler, "A new framework for detailed electrochemical modeling of solid oxide fuel cells," Electrochim. Acta **53**, 1782-1800 (2007).
14. S. Gewies and W. G. Bessler, "Physically based impedance modeling of Ni/YSZ cermet anodes", J. Electrochem. Soc., submitted (2008).
15. M. Vogler, A. Bieberle-Hütter, L. J. Gauckler, J. Warnatz, and W. G. Bessler, "Towards understanding the elementary kinetics of hydrogen oxidation at Ni/YSZ model anodes," Solid State Ionics, submitted (2008).
16. H. Zhu, R. J. Kee, V. M. Janardhanan, O. Deutschmann, and D. G. Goodwin, "Modeling elementary heterogeneous chemistry and electrochemistry in solid-oxide fuel cells," J. Electrochemical Soc. **152**, A2427-A2440 (2005).
17. P. Metzger: *Charakterisierung von oxidkeramischen Festelektrolyt-Brennstoffzellen durch ortsaufgelöste Messungen*, Ph.D. Thesis, Universität Stuttgart, Stuttgart, (2006).
18. S. Gewies, W. G. Bessler, J. Warnatz, V. Sonn, and E. Ivers-Tiffée, "Coupled electrochemistry and transport in Ni/YSZ cermets: Impedance simulations and experimental validation," in *Proceedings of the 7th European Solid Oxide Fuel Cell Forum*, Lucerne, Switzerland, P0713 (2006).